Published in final edited form as:
Clin Cancer Res. 2011 May 15; 17(10): 3134–3145. doi:10.1158/1078-0432.CCR-10-2443.

Enhancement of T-cell mediated anti-tumor response: angiostatic adjuvant to immunotherapy against cancer

Ruud P.M. Dings[*], **Kieng B. Vang**[#], **Karolien Castermans**[%], **Flavia Popescu**[#], **Yan Zhang**[&], **Mirjam G. A. oude Egbrink**[~], **Matthew F. Mescher**[#], **Michael A. Farrar**[#], **Arjan W. Griffioen**[%], and **Kevin H. Mayo**[*,$]

[*]Department of Biochemistry, Molecular Biology & Biophysics, University of Minnesota, U.S.A. [#]Department of Laboratory Medicine and Pathology, Center for Immunology, University of Minnesota, U.S.A. [&]Department of Biostatistics Core, The Masonic Cancer Center, University of Minnesota, U.S.A. [%]Angiogenesis Laboratory, School for Oncology and Developmental Biology (GROW), Department of Pathology, Maastricht University and University Hospital, Maastricht, The Netherlands [~]Physiology, Maastricht University and University Hospital, Maastricht, The Netherlands

Abstract

Purpose—Tumor-released pro-angiogenic factors suppress endothelial adhesion molecule (EAM) expression and prevent leukocyte extravasation into the tumor. This is one reason why immunotherapy has met with limited success in the clinic. We hypothesized that overcoming EAM suppression with angiogenesis inhibitors would increase leukocyte extravasation and subsequently enhance the effectiveness of cellular immunotherapy.

Experimental Design—Intravital microscopy, multiple-color flow cytometry, immunohistochemistry, and various tumor mouse (normal and T cell-deficient) models were used to investigate the temporal dynamics of cellular and molecular events that occur in the tumor microenvironment during tumor progression and angiostatic intervention.

Results—We report that while EAM levels and T cell infiltration are highly attenuated early on in tumor growth, angiostatic therapy modulates these effects. In tumor models with normal and T cell-deficient mice, we demonstrate the active involvement of the adaptive immune system in cancer, and differentiate anti-angiogenic effects from anti-angiogenic-mediated enhancement of immuno-extravasation. Our results indicate that a compromised immune response in tumors can be obviated by the use of anti-angiogenic agents. Lastly, with adoptive transfer studies in mice, we demonstrate that a phased combination of angiostatic therapy and T cell transfer significantly ($P<0.0013$) improves tumor growth inhibition.

Conclusions—This research contributes to understanding the cellular mechanism of action of angiostatic agents and the immune response within the tumor microenvironment, in particular as a

[$]To whom correspondence should be addressed: Dr. K. H. Mayo, Dept. of Biochemistry, 6-155 Jackson Hall, University of Minnesota Health Sciences Center, 321 Church Street, Minneapolis, Minnesota 55455, USA, Phone: 612-625-9968; Fax: 612-624-5121; mayox001@tc.umn.edu.

consequence of the temporal dynamics of EAM levels. Moreover, our results suggest that adjuvant therapy with angiogenesis inhibitors holds promise for cellular immunotherapy in the clinic.

Keywords

tumor microenvironment; adaptive immune system; angiogenesis; endothelial cell anergy; anginex

Introduction

Although the immune system can recognize and eliminate tumors (1), many cancers escape host immunity, as evidenced annually by the number of cancer associated deaths (2). In addition, although cellular immunotherapy initially showed great promise in pre-clinical trials, it has yet to fulfill this promise in the clinic (3). For insight into this apparent conundrum, we investigate endothelial cell (EC) anergy as a novel mechanism by which tumors can escape immuno-surveillance and subsequently impede effects from immunotherapy. EC anergy is defined as the down regulation of EC adhesion molecules (EAMs) [e.g. intercellular adhesion molecule 1 (ICAM-1), vascular cell adhesion molecule (VCAM-1), and E-selectin] (4). EAMs are crucial for leukocyte extravasation into the tumor, and their expression can be suppressed by pro-angiogenic factors, like vascular endothelial growth factor (VEGF) and fibroblast growth factor (FGF) (5–7). Therefore, we hypothesized that inhibition of angiogenesis (using anti-angiogenic agents) will overcome growth factor-induced EAM suppression and lead to normalized EAM levels. This, in turn, should promote vascular rolling, adherence, and transmigration of leukocytes into tumor tissue, making tumors more vulnerable to host immunity. More importantly, since cellular immunotherapy relies heavily on leukocyte extravasation into the tumor, we hypothesized that normal vascular EAM levels in the tumor microenvironment should increase the effectiveness of adoptive immunotherapy.

Anginex, a designer peptide 33mer, has been shown to target galectin-1 (gal-1), a novel player in antiangiogenesis research (8, 9). We and others have shown that the interaction between anginex and galectin-1 inhibits tumor-activated endothelial cell proliferation via anoikis (10) and attenuates tumor angiogenesis and tumor growth (11, 12). By weakly binding to ‘carrier protein’ plasma fibronectin (11), anginex is transported through the cardiovascular system to the tumor where the peptide strongly binds gal-1 (K_d = 90 nM) (8). We have previously demonstrated that this peptide can synergistically enhance the effects of chemotherapeutics and radiotherapy in several solid tumor types (13–15).

Here we demonstrate that anginex and its topomimetic 0118 (15, 16) can counteract pro-angiogenic factor-induced EAM suppression and promote T cell specific anti-tumor immunity. By treating B16F10 melanoma and Lewis Lung Carcinoma (LLC) tumor-bearing mice ($CD4^{-/-}$ and $CD8^{-/-}$ vs. wild type) with these angiogenesis inhibitors, we differentiated anti-angiogenic from immuno-extravasation enhancement effects. Additionally the temporal dynamic changes in EAM levels and T cell extravasation during tumor progression and therapeutic intervention were simultaneously elucidated, and we revealed that increased immuno-extravasation accounted for up to 70% of tumor growth inhibition at early time points post initiation of angiogenic therapy. Subsequently, adoptive

immuno-transfer studies demonstrated that immunotherapy administered within this angiogenic therapy-initiated time window significantly increased tumor growth inhibition. Overall, our work strongly suggests that adjuvant therapy with angiogenesis inhibitors holds promise for immunotherapy in the clinic.

Materials and Methods

Cell culture

Human umbilical vein-derived endothelial cells (HUVEC), mouse B16F10 melanoma cells (kindly provided by Dr. Isaiah J. Fidler, Houston, TX), Lewis lung adenocarcinoma (LLC; ATCC, Manassas, VA) and the human epithelial ovarian carcinoma cell line, MA148 (kindly provided by Prof. Dr Ramakrishnan, Minneapolis, MN) were cultured as previously described (17).

Quantitative real time RT-PCR (qRT-PCR)

Total RNA isolation from cultured cells or from tumor tissue, cDNA synthesis and quantitative real-time RT-PCR were performed essentially as described previously using SYBR Green PCR master mix (Eurogentech, Liege, Belgium) spiked with 20nM fluorescein (Bio-Rad, Veenendael, The Netherlands) (18). The expression of each target gene was normalized to the expression of the control gene beta-actin. Species-specific primers can be found in Table S2.

Intravital microscopy

B16F10 tumors were grown in the flank of C57BL/6 mice by s.c. injection of 1×10^5 cells in 100μl in 0.9% NaCl solution. Mice were treated (10 mg/kg/day, BID i.p.) daily for 2 days with anginex (n=7) or 0118 (n=8) or vehicle (n=6) when tumors had a volume of about 80 mm^3 and imaged the day after. To enable intravital microscopic observations of leukocytes, 10–20 μl of a Rhodamine 6G solution (1 mg/ml in 0.9% NaCl solution) was injected i.v. via tail vein, as described before (19).

Mice and tumor mouse models

All mice used in this study [C57BL/6J, $CD8^{-/-}$ null (B6.129S2-Cd8a^{tm1Mak}/J); $CD4^{-/-}$ null (B6.129S6-Cd4^{tm1Knw}/J); $CD8^{-/-}CD4^{-/-}$ null (B6.Cg-Foxn1^{nu}/J); or athymic nude nu/nu] were purchased from Jackson Laboratory (Bar Harbor ME) and allowed to acclimate to local conditions for at least 1 week. Forkhead box N-1 (Foxn-1) null mice have a mutation in the nude locus that affects normal thymus development, resulting in T cell immunodeficiency. Animals were provided water and standard chow *ad libitum* and were maintained on a 12-h light/dark cycle. Experiments were approved by the University of Minnesota Research Animal Resources ethical committee. For tumor cell inoculation, a 100 μL solution of 2×10^5 of B16F10 or 1×10^6 LLC were injected subcutaneously in the right rear leg of the mice. For the human ovarian MA148 carcinoma studies, female athymic nude mice were subcutaneously inoculated with 2×10^6 MA148 cells into the right flank, as described previously (17). Wild type and null mice (sex- and age-matched littermates) were randomly inoculated and were randomized again prior to the initiation of treatment. Tumor volume was determined by measuring the diameters of tumors with calipers and calculated by the

equation for volume of a spheroid: $(a^2 \times b \times \pi)/6$, were *a* is the width and *b* the length of the tumor. When tumors reached a volume of approximately 100 mm^3 (approximately 7 days for B16F10, 10 days for LLC and 40 days for MA148), treatment was initiated by administering anginex or 0118 (10 mg/kg/day IP BID), as described previously (16). In most studies, treatment was administered daily for 8 to 10 days to the end of the study. For adoptive immuno transfer studies (Figure 7), treatment was administered for only 2 days, as described in the text.

Flow Cytometry and FACS analysis - In vitro cultures

HUVEC were cultured for 3 days with or without growth factors bFGF, VEGF and different concentrations of angiogenesis inhibitors anginex, or topomimetics 0118, 1049, 1097 which were synthesized and purified as described previously (16). For the detection of VCAM-1 and E-selectin, 4ng/ml TNFα (PeproTech Inc., Rocky Hill, NJ) was added 6 hours prior to harvesting. Cells were trypsinized and fixed with 1% paraformaldehyde for 30min at room temperature. ICAM-1, VCAM-1 and E-selectin expression was detected by anti-human ICAM-1 (MEM111, Monosan, Uden, The Netherlands), VCAM-1 (1G11, Hbt, Uden, The Netherlands) or E-selectin (ENA-1, a kind gift from Dr. W.A. Buurman, Maastricht University, The Netherlands). Followed by incubation with biotin conjugated rabbit anti-mouse IgG and Strep-PE (both DAKO, Glostrup, Denmark).

In vivo studies

Tumors were harvested and were non-enzymatically disrupted by shear force to yield single cell suspensions (20) on the days indicated. Treatment with 0118 (10 mg/kg IP BID) was initiated on day 10, and from that day on, size-matched tumors were excised at time points indicated. Anti-mouse antibodies CD54-PE, CD106-FITC, CD31-PE, CD31-FITC, CD31-PE-Cy7, CD34-pacifin blue, aSMA- FITC, CD45-PECy5.5, CD45-FITC, CD3-PE, CD8a-biotin, CD8a-APC Alexa fluor 750, CD4-biotin, CD4-Alexa fluor 700, CD69-biotin, streptavidin-APC, and isotype controls were purchased from eBioscience (San Diego, CA) and used for either FACS analysis or immunofluorescense. Intracellular Foxp3 and granzyme B staining was done, as described before (20). FITC labeled anti-mouse antibodies (eBioscience) for macrophages/ monocytes/ granulocytes (CD11b), NK cells (NK1.1), erthrocytes (Ter119), macrophages (Gr-1), and B cells (CD19), were used to create an exclusion channel. Samples were analyzed by multi-parameter flow cytometry on a LSR II flow cytometer (BD Biosciences, San Jose, CA) using Flowjo software (Tree Star Ashland, OR) (20).

T cell adoptive immunotherapy in mice

When B16F10 tumors reached an approximate size of 75 mm^3 [in either C57BL/6 or Foxn-$1^{-/-}$ mice], 0118 (10 mg/kg/day IP BID) treatment was initiated for 2 days. On day 7, 2×10^7 T cells (16.8% CD4, 23.5% CD8, and 56.2% DPs), were transferred IP per mouse. The T cells were derived from thymii and spleens of age- and sex-matched C57BL/6 wild type littermates by MACS beads purification (Miltenyi Biotech, Auburn, CA), according the manufacturer's instructions. Since reports have shown that transfers of activated T cells can actually impair the anti-tumor efficacy (21), T cell transfers in our model were executed

with non-stimulated/ non-activated T cells. Due to the aggressive growth rate of B16F10 only one adoptive transfer is possible (21). Moreover, in our case the transfer had to be preceded by two days of angiostatic treatment without interfering with tumor establishment.

Immunofluorescence

Immunofluorescence stainings were performed on acetone fixed cryo-sections (5 μm). Images of the sections were acquired on Olympus BX-60 microscope at 200× magnification and digitally analyzed and differentially quantified by morphometric analysis, as described earlier (16).

Statistical analysis

Tumor volume data were first transformed into a natural log scale, then those related to Supplemental Figure S3 were analyzed using analysis of variances (ANOVA) due to factorial design, and those related to Figures 5, 7 and Supplemental Figure 4 were analyzed using general linear mixed models for repeated measures as described previously (16). For the latter type of analysis, the likelihood ratio test was used to determine variance-covariance structures and model components, and only the linear time trend was considered.

Raw data of tumor volume related to Figure 5, 6 and Supplement Figure 4 were also analyzed in their original scale using the general linear mixed model for repeated measures, in which both linear and quadratic time trends were considered. Using the estimates of model parameters, model-based tumor growth curves for raw data were drawn and the area under the curve was calculated via integration. This integral provided estimates of percentage inhibition in tumor growth for treatment versus reference groups over the time course of the study, rather than just on a single day.

The Student's *t* test was used where indicated to determine the validity of differences between control and treatment data sets. A *p* value of 0.05 or less was considered significant.

Online supplemental material

Fig. S1 shows quantifications of images from intravital fluorescence microscopy using rhodamine-labeled leukocytes in healthy tissue or in treated or untreated B16F10 tumors. Fig. S2 shows the effects of angiostatic treatment on circulating leukocytes. Fig. S3 shows tumor progression in different strains of T cell deficient mice. Fig. S4 shows tumor progression in different strains of T cell deficient mice with and without angiostatic treatment. Fig. S5 shows the reduction in tumor endothelial cells by 0118 treatment. Table S1 shows the fluid dynamic parameters in tumor vessels of treated and non-treated mice. Table S2 shows the murine-specific sequences of primers used in the quantitative real-time RT-PCR.

Results

Overcoming EC anergy promotes leukocyte-vessel interactions in tumors

Here we show that the gal-1-targeted designer peptide anginex, partial peptide 6DBF7, and its calixarene-based topomimetic 0118 (12), as well as tyrosine kinase inhibitors Gleevec (imatinib) and Tarceva (erlotinib), were able to normalize ICAM-1 expression on cultured human EC (Figure 1A).

On the other hand, non-angiostatic calixarene analogs of 0118 (1049 and 1097) showed no significant effect on ICAM-1 normalization in this assay. Furthermore, the increase of ICAM-1 protein was also revealed at the transcription level, as evidenced by mRNA levels for ICAM-1, VCAM-1, and E-selectin, using real-time quantitative RT-PCR with anginex and 0118 (Fig. 1B).

To assess real time leukocyte-endothelium interactions *in vivo*, we used intravital microscopy on B16F10 tumor-bearing mice. Exemplary still shots are provided in Figure 1C.[1] While leukocyte-vessel wall interactions in tumors of control mice are significantly reduced ($P<0.01$) compared to those in normal tissue (Fig. S1; Supplemental Information), leukocyte-vessel wall interactions are increased by about 3-fold treatment in tumors of mice treated with anginex or 0118 (Fig. 1D), without inducing such changes in normal tissue of the ear (Fig. S1). Quantification of the interactions allows differentiation of adhered and rolling leukocytes, both of which are increased in tumor vessels as the result of angiostatic therapy (Fig. 1E and 1F). These observations were not the result from leukocyte activation or mobilization (Fig. S2), altered expression of leukocyte adhesion molecules LFA-1α, LFA-1β, VLA-4, or L-selectin on peripheral blood leukocytes (data not shown), or reduced blood flow velocity (Table S1).

EAM levels during tumor growth

Because of the plasticity of the tumor microenvironment during cancer progression (22), we hypothesized that EAM levels, and consequently T-cell infiltration, have a dynamic temporal component. As shown by flow cytometry, ICAM-1 (Fig. 2A) and PECAM (Fig. 2C) levels were reduced during tumor growth, whereas average VCAM levels (Fig. 2B) appeared unchanged.

To assess the temporal effect of anti-angiogenesis therapy on EAM levels, we treated a randomized subset of mice with angiostatic compound 0118 (10 mg/kg IP, BID) starting on day 10 post-inoculation when the average tumor size was 100 mm^3, in order to prevent concerns with tumor take. Treatment was administered daily to the end of the study. EAM levels on tumor EC in treated mice increased on average by about 2-fold, compared to untreated controls with size-matched tumors (Fig. 2A–C). We substantiated this in an independent experiment, where immunohistochemical analysis revealed a significant increase ($P<0.05$) in ICAM-1 positive blood vessels ($CD54^+CD31^+$) in treated B16F10 tumor tissue over vehicle treated controls (Fig. 2D). Moreover, by using mouse-specific

[1]Video images of vessels from these experiments can be viewed at http://www.fdg.unimaas.nl/angiogenesislab/Mirrorsite/castermans%20movies.htm

primers (Table S2) in a human xenograft model (MA148, ovarian cancer; (16)), we quantified mouse-specific ICAM-1 mRNA expression, which increased nearly 2-fold in mice treated with either anginex or 0118 (Fig. 2E and Table S2).

T cell infiltration and activation during tumor growth

In untreated mice, the T cell decrease observed during tumor growth (Fig. 3A and 3B) parallels the decrease in EAM levels on tumor EC (Fig. 2). However, while the number of $CD4^+$ cells decreases seemingly monotonically during tumor growth (Fig. 3A), the $CD8^+$ cell population remains roughly constant up to day 12, peaks on day 13, and then falls below initial levels by the end of the study (Fig. 3B). Assessment of the early activation marker CD69 indicates that a portion of these T cells is activated. Up to day 7, the number of $CD69^+$ cells accounts for about 10% of the $CD4^+$ and $CD8^+$ populations, which subsequently increases to about 30% and peaks at about 70% by day 12 or 13 (Fig. 3A and 3B). Treatment with 0118 leads to a 2-fold increase in the number of $CD4^+$ (Fig. 3C) and $CD8^+$ cells (Fig. 3D), with exemplary FACS dot plots in Figure 3G. The angiogenic therapy-related increase in T cell infiltration parallels the increase in EAM levels (Fig. 2). We also observed that angiogenic therapy promoted about a 2-fold increase in the number of $CD69^+$ cells within both the $CD4^+$ (Fig. 3E) and $CD8^+$ (Fig. 3F) populations, with exemplary FACS dot plots in Figure 3G.

T cell activation was also verified in a separate flow cytometry study that included assessment of blast phenotype, and the expression of CD69 and granzyme B. In this single time point study (15 days post inoculation that included 5 days of treatment), we found that about 40% of the $CD8^+$ cell population in untreated tumors expressed CD69 and about 15% of these cells displayed a blast phenotype (Fig. 4A). In addition, about 50% of these T cells expressed granzyme B (Fig. 4A), suggesting potential cytotoxicity against tumor cells. Although angiostatic treatment did not alter the percent of activation within the $CD8^+$ cell population (Fig. 4A), it did increase the total amount of infiltrated activated $CD8^+$ cells (Fig. 4B).

Regulatory T cells (Tregs, $CD4^+Foxp3^+$) control and dampen the induction and effector phase of the immune defense system (23). Even though treatment with 0118 lead to a 2-fold increase in overall $CD4^+$ cells (Fig. 3C), the percentages of Tregs were comparable (about 1%) between untreated and 0118 treated mice, indicating that 0118 does not promote formation of Tregs (Fig. 4C).

Quantifying immune enhancement during angiostatic therapy

So far, our data demonstrate that angiostatic therapy with anginex or 0118 has a dual mechanism of action. Although its traditionally accepted mechanism of action is to reduce vessel density in tumors (Fig. S5 and references (15, 16)), we now know that it also promotes T cell infiltration into tumors by counteracting EC anergy. To differentiate the effects on tumor growth from an angiogenesis inhibitor and angiogenesis inhibitor-mediated immuno-extravasation, we used $CD8^{-/-}$ and $CD4^{-/-}$ null mice with B16F10 or LLC tumors. Because tumor growth is delayed in wild type compared to null mice (Fig. S3), we initiated angiostatic treatment in either cohort when tumors were about 100 mm^3 (i.e. to have size-

matched tumors and not to interfere with tumor take). Tumor growth curves are shown for B16F10 in $CD8^{-/-}$ and wild type mice (Fig. 5A). Tumor growth curves for B16F10 in $CD4^{-/-}$ and wild type mice and for LLC in $CD8^{-/-}$ and wild type mice can be found in the Supplemental Information (Fig. S4).

Statistical analysis of tumor volume data using general linear mixed models showed that B16F10 tumor growth was significantly inhibited up to 2.5 fold in $CD8^{-/-}$ mice treated with anginex (P=0.0316) or 0118 (P=0.0222) on the last day of treatment (Fig. 5A). Whereas in wild type mice, tumor growth was more significantly inhibited (anginex (P=0.0009) and 0118 (P=0.0018). Comparable results were obtained for B16F10 tumors by 0118 in $CD4^{-/-}$ mice (P=0.0553) compared to wild type mice (P=0.03, Fig. S4). As well as in the LLC tumor model, where on the last day of treatment LLC tumor growth was significantly inhibited in $CD8^{-/-}$ mice treated with anginex (P=0.0367) or 0118 (P=0.0118; Fig. S4), as compared to the tumor growth inhibition of anginex (P<0.0001) or 0118 (P=0.0062) in wild type mice (Fig. S4).

Using the area-under-the-curve approach (9), we calculated tumor growth inhibition over the entire time of treatment based on the estimated tumor growth curves of raw data. Taken together, angiostatic treatment inhibited tumor growth on average by 65% (±5.4%) in wild type mice compared to 44% (±3.6%) in null mice (P=0.01). These results indicate that the angiostatic-mediated increase in leukocyte infiltration into tumors accounts for a time-averaged tumor growth inhibitory effect of 32% (21/65).

However, if we analyze the effect on a daily basis, we find that the immuno-extravasation effect can be as high as 70% initially, and as low as 10% by the end of the study. For this, we calculated the daily fraction of tumor growth inhibition (i.e. tumor size in anginex or 0118 treated mice divided by that in untreated mice) in null mice divided by the fraction of tumor growth inhibition in wild type mice. One minus this ratio times 100 yields the percent enhancement, which is plotted vs. time in Figure 5B for all tumor models investigated. The immuno-extravasation effect is greatest at the onset of treatment, and then declines to the end of the study. We found essentially the same trend in each tumor model, and linear fits to these data indicate highly significant correlations with a regression coefficient R = 0.92 for all data with 0118, and R = 0.90 for all data with anginex.

Enhancement of adoptive immunotherapy

To demonstrate feasibility, we performed an adoptive immunotherapy study in which we treated B16F10 tumor-bearing T-cell deficient ($Foxn1^{-/-}$) and wild type control mice with 0118 for only 2 days, followed by adoptive transfer of isolated T cells. Since reports have shown that transfers of effector T cells can actually impair the anti-tumor efficacy (21), T cell transfers in our model were executed with non-stimulated/ non-activated T cells. Angiostatic treatment (10 mg/kg IP, BID) was initiated when tumors reached approximately 70 mm^3 and was administered only for two days, days 5 and 6 (in contrast to the 8 days of treatment in Figure 6). The adoptive transfer of 2×10^7 T cells (16.8% CD4, 23.5% CD8, and 56.2% double positives) was administered on day 7.

The two days of angiostatic therapy alone showed no significant effect on tumor growth in both the Foxn1$^{-/-}$ and wild type mice, whereas the adoptive transfer alone inhibited tumor growth by about 50% on the last day in Foxn1$^{-/-}$ mice (Fig. 6A). However, the greatest effect resulted from the staggered combination of both therapies, where tumor growth was inhibited by about 70% in Foxn1$^{-/-}$ mice (P=0.0015) with significant improvement over 0118 (P=0.0144) and marginally significant improvement over T cells alone (P=0.089) on the last day of treatment (Fig. 6A); and by around 90% in wild type mice (P<0.0001) with significant improvement over the monotherapies (P<0.0001 vs 0118, and P=0.0013 vs T cells) on the last day of treatment (Fig. 6B).

As proof that T cells from the adoptive transfer indeed infiltrated into tumors of Foxn1$^{-/-}$ mice, we observed a significant (p<0.01) increase in T cells in the combination-treated mice, compared to adoptive T cell transfer alone (Fig. 6C and 6E). No CD45^{+}CD3^{+} cells were detected in vehicle-treated or 0118 treated mice, as these mice did not receive a T cell transfer (Fig. 6E), and the CD45^{+} cells present in vehicle and 0118 treated mice (Fig. 6D), likely arising from other types of leukocytes, e.g. macrophages, present in Foxn1$^{-/-}$ mice.

Discussion

The causal relationship between inflammation, immune response, and cancer has now been widely accepted (22). However, the precise involvement of the tumor microenvironment, in particular tumor EC, remains largely unclear. Various types of immunosuppression and tolerance have been associated with the tumor microenvironment, which can impede adequate T cell effector function, e.g. co-inhibitory effects of cytokines on activation, proliferation, and survival of T cells (24), interference with migration of activated T cells to the tumor due to lack of tumor chemokine or T cell chemokine receptor expression (3), or suppression of T cell effector function by Tregs, TGF-β, or iNos (23). These immunosuppressive mechanisms occur at different stages of the T cell response and have been suggested as possible reasons for the limited success of T cell-based immunotherapy (3). Here, we investigate the downregulation of EAM levels as a novel mechanism of immunosuppression through which tumors can escape immuno-surveillance and attenuate effects from immunotherapy.

Angiogenesis is postulated to contribute to the escape of tumors from host immunity by modulating EAMs and thereby reducing leukocyte-vessel wall interactions and subsequent infiltration (5, 6). For example, in response to angiogenic growth factors, EAMs display an acute temporal upregulation within hours (25), after which the expression levels fall below the initial baseline around day 2 (6, 7, 25–27). The exposure to pro-angiogenic stimuli for an extended period of time, e.g. >24 hours *in vitro* or as we show here in an *in vivo* setting such as a tumor, results in the downregulation of EAMs and subsequent reduced leukocyte-endothelium interactions. In our tumor mouse models, we demonstrate that these dynamic changes in EAM levels are most pronounced on ICAM-1 and PECAM levels, which are decreased by about 50% during tumor growth, whereas VCAM levels appear on average to remain constant. Mechanistically, it has been shown that angiogenesis growth factor-mediated suppression of ICAM-1 results from inhibition of phosphorylation and degradation of IkB, the natural inhibitor of NFκB (28), and that upregulation of ICAM-1 in tumor EC

occurs via epigenetic mechanisms, primarily at the level of histone deacetylation of tumor endothelial genes (29). Angiogenesis inhibitors such as anginex, angiostatin and endostatin have been shown to upregulate NFκB and subsequent ICAM-1 levels, whereas Avastin (bevacizumab) failed to do so (30).

Additionally, we demonstrate that tumor progression occurs more rapidly in T cell-compromised mice, indicating that the adaptive immune system should be important in cancer. Nevertheless, this is apparently insufficient, as the tumor still progresses and the amount of (activated) T cells decreases over time. This suggests that the T cell-mediated response is hampered by tumor-induced counter measures, such as down regulation of EAMs, i.e. EC anergy. We show here that angiostatic treatment abrogates growth factor-induced suppression of EAMs and specifically facilitates host immunity by promoting T cell adhesion to tumor EC and subsequent infiltration into the tumor. Furthermore, we found that the number of activated effector T cells with specific anti-tumor activity is significantly increased upon angiostatic therapy. The tumor growth inhibition differential effect of angiostatic treatment in tumor-bearing CD8 and CD4 null mice compared to wild type also argues for specific anti-tumor immunity.

Whereas innate immune cells have been shown to promote tumorigenesis in certain instances (31), the adaptive immune system generally exhibits anti-tumor effects. Most studies conclude that an increase in T-lymphocytes in tumor tissue improves patient survival (32, 33), yet some studies report that substantial lymphocyte infiltration promotes tumor progression (34). This apparent contradiction may be explained by considering the state of T cell activation and the cytolytic capacity of tumor-infiltrated lymphocytes (35). In addition, tumor specific CD4 T cells appear to be functionally manifold, since they help or hinder anti-tumor immune responses (23). E.g. in a MMTV-PyMT model, $CD4^+$ T cells had no effect on primary mammary tumor growth or angiogenesis, but they did enhance the number of pulmonary metastasis through the innate involvement of macrophages (36). Moreover, $CD4^+$ T cells can give rise to Tregs. In this regard Tregs are undesirable, because Tregs prevent induction of tumor-associated antigen-specific immunity and inhibit the effector function of cytotoxic T cells and NK cells (3, 37). Additionally, Tregs express ectoenzymes CD39/ENTPD1 and CD73/ecto-5′-nucleotidase, which generate pericellular immunosuppressive adenosine from extracellular nucleotides via degradation of ATP to AMP (38). This is supported by the observation that the inactivation of the A_{2A} adenosine receptor rescues endogenous anti-tumor T-cell responses and induces successful tumor rejection (39). Therefore, the coordinated expression and cross talk of CD39/CD73 on Tregs and the adenosine A_{2A} receptor on activated T effector cells generates immunosuppressive loops, inhibiting optimal anti-tumor immune responses. Although the amount of Tregs in our tumor models is low (1%), blocking Treg function would likely further improve the anti-tumor effects, since studies have demonstrated that anti-tumor therapy can be improved by removal of this immunoregulatory host mechanism to permit a robust, persistent immune response in the tumor (40, 41).

Adoptive immunotherapy has been around for some time, but has yet delivered on its promise to the clinic. Thus far, this has been explained in part by the generally unaccommodating nature of the tumor microenvironment, such as an aberrant vascular bed,

oxidative stress, high lactate levels, low pH, and high interstitial fluid pressure. Here, we demonstrate that antiangiogenic agents can improve certain conditions in the tumor microenvironment by upregulating EAMs and promoting leukocyte infiltration into tumor tissue. Because we found that angiostatic-induced increase in leukocyte infiltration into tumors accounts for a time-averaged tumor growth inhibitory effect of about one-third, the remaining two-thirds should be attributable to the direct anti-angiogenic effect. These two effects occur in a time dependent manner, with the immuno-extravasation effect being greater (up to 70%) at early time points following initiation of treatment, and becoming less as the anti-angiogenic effect increases. The timeline of this effect and its peak occurrence within several days post initiation of angiostatic treatment essentially parallels that observed in our earlier study which demonstrated anginex- and 0118-induced tumor vessel maturation (17). With this in mind, one might argue that angiostatic treatment, which can temporally improve overall tumor physiology may be responsible for the increase in tumor infiltrate. Yet, the increase in the number of activated T cells argues for an active, rather than for a passive effect, such as vessel normalization. Additionally, no reduced blood flow velocity or blood pressure was noted upon treatment (14). Also, our results can not be explained by a direct effect on leukocytes themselves, as angiostatic therapy did not change the level of activation, nor did it change the ratio of infiltrating activated to non-activated leukocytes. Furthermore, the number of circulating leukocytes in peripheral blood was unaffected by angiostatic treatment, and the expression of leukocyte adhesion molecules was also not altered. Overall, our work strongly suggests that overcoming EC anergy by adjuvant therapy with angiogenesis inhibitors holds promise for immunotherapy in the clinic.

Translational relevance

Our studies demonstrate the active involvement of the adaptive immune system in tumors, and indicate that a compromised immune response in tumors can be obviated by the use of an anti-angiogenic agent. Moreover, our results strongly suggest that adjuvant therapy with angiogenesis inhibitors (administered within an appropriate time frame) holds promise for cellular immunotherapy in the clinic.

Supplementary Material

Refer to Web version on PubMed Central for supplementary material.

Acknowledgments

We thank Dr. Paul Champoux for the assistance with flow cytometry and Dr. Xianghua Luo and Ms. Xiao Liu for assistance with statistical analysis. This research was supported by research grants to KHM from the National Cancer Institute (NIH CA-096090) and a research supplement to promote diversity in health related research (to KBV).

RPMD, KC, MGAE, MFM, MAF, AWG and KHM designed the research and analyzed the data. RPMD, KBV, KC, FP executed the research. YZ statistically analyzed the data.

KHM has a financial interest in a pharmaceutical company that holds license to commercialize agents (anginex and 0118) investigated in this manuscript.

Abbreviations

EC	endothelial cell
EAM	endothelial adhesion molecule
HUVEC	human umbilical vein EC
PBS	phosphate buffered saline

References

1. Dunn GP, Old LJ, Schreiber RD. The three Es of cancer immunoediting. Annu Rev Immunol. 2004; 22:329–360. [PubMed: 15032581]
2. Parkin DM, Bray F, Ferlay J, Pisani P. Global cancer statistics, 2002. CA Cancer J Clin. 2005; 55:74–108. [PubMed: 15761078]
3. Lizee G, Cantu MA, Hwu P. Less yin, more yang: confronting the barriers to cancer immunotherapy. Clin Cancer Res. 2007; 13:5250–5255. [PubMed: 17875752]
4. Griffioen AW, Damen CA, Mayo KH, et al. Angiogenesis inhibitors overcome tumor induced endothelial cell anergy. Int J Cancer. 1999; 80:315–319. [PubMed: 9935216]
5. Griffioen AW, Damen CA, Blijham GH, Groenewegen G. Tumor angiogenesis is accompanied by a decreased inflammatory response of tumor-associated endothelium. Blood. 1996; 88:667–673. [PubMed: 8695814]
6. Melder RJ, Koenig GC, Witwer BP, Safabakhsh N, Munn LL, Jain RK. During angiogenesis, vascular endothelial growth factor and basic fibroblast growth factor regulate natural killer cell adhesion to tumor endothelium. Nat Med. 1996; 2:992–997. [PubMed: 8782456]
7. Tromp SC, oude Egbrink MG, Dings RP, et al. Tumor angiogenesis factors reduce leukocyte adhesion in vivo. Int Immunol. 2000; 12:671–676. [PubMed: 10784613]
8. Thijssen VL, Postel R, Brandwijk RJ, et al. Galectin-1 is essential in tumor angiogenesis and is a target for antiangiogenesis therapy. Proc Natl Acad Sci U S A. 2006; 103:15975–15980. [PubMed: 17043243]
9. Dings RP, Van Laar ES, Loren M, et al. Inhibiting tumor growth by targeting tumor vasculature with galectin-1 antagonist anginex conjugated to the cytotoxic acylfulvene, 6-hydroxylpropylacylfulvene. Bioconjug Chem. 2010; 21:20–27. [PubMed: 20020769]
10. Griffioen AW, van der Schaft DW, Barendsz-Janson AF, et al. Anginex, a designed peptide that inhibits angiogenesis. Biochem J. 2001; 354:233–242. [PubMed: 11171099]
11. Akerman ME, Pilch J, Peters D, Ruoslahti E. Angiostatic peptides use plasma fibronectin to home to angiogenic vasculature. Proc Natl Acad Sci U S A. 2005; 102:2040–2045. [PubMed: 15687502]
12. Dings RP, Mayo KH. A journey in structure-based drug discovery: from designed peptides to protein surface topomimetics as antibiotic and antiangiogenic agents. Acc Chem Res. 2007; 40:1057–1065. [PubMed: 17661438]
13. Dings RP, Yokoyama Y, Ramakrishnan S, Griffioen AW, Mayo KH. The designed angiostatic peptide anginex synergistically improves chemotherapy and antiangiogenesis therapy with angiostatin. Cancer Res. 2003; 63:382–385. [PubMed: 12543791]
14. Dings RP, Williams BW, Song CW, Griffioen AW, Mayo KH, Griffin RJ. Anginex synergizes with radiation therapy to inhibit tumor growth by radiosensitizing endothelial cells. Int J Cancer. 2005; 115:312–319. [PubMed: 15688384]
15. Dings RP, Van Laar ES, Webber J, et al. Ovarian tumor growth regression using a combination of vascular targeting agents anginex or topomimetic 0118 and the chemotherapeutic irofulven. Cancer Lett. 2008; 265:270–280. [PubMed: 18378392]
16. Dings RP, Chen X, Hellebrekers DM, et al. Design of nonpeptidic topomimetics of antiangiogenic proteins with antitumor activities. J Natl Cancer Inst. 2006; 98:932–936. [PubMed: 16818857]

17. Dings RP, Loren M, Heun H, et al. Scheduling of radiation with angiogenesis inhibitors Anginex and Avastin improves therapeutic outcome via vessel normalization. Clin Cancer Res. 2007; 13:3395–3402. [PubMed: 17545548]
18. Thijssen VL, Brandwijk RJ, Dings RP, Griffioen AW. Angiogenesis gene expression profiling in xenograft models to study cellular interactions. Exp Cell Res. 2004; 299:286–293. [PubMed: 15350528]
19. Dirkx AE, oude Egbrink MG, Castermans K, et al. Anti-angiogenesis therapy can overcome endothelial cell anergy and promote leukocyte-endothelium interactions and infiltration in tumors. Faseb J. 2006; 20:621–630. [PubMed: 16581970]
20. Vang KB, Yang J, Mahmud SA, Burchill MA, Vegoe AL, Farrar MA. IL-2, -7, and -15, but not thymic stromal lymphopoeitin, redundantly govern CD4+Foxp3+ regulatory T cell development. J Immunol. 2008; 181:3285–3290. [PubMed: 18714000]
21. Gattinoni L, Klebanoff CA, Palmer DC, et al. Acquisition of full effector function in vitro paradoxically impairs the in vivo antitumor efficacy of adoptively transferred CD8+ T cells. J Clin Invest. 2005; 115:1616–1626. [PubMed: 15931392]
22. Coussens LM, Werb Z. Inflammation and cancer. Nature. 2002; 420:860–867. [PubMed: 12490959]
23. Sakaguchi S. Naturally arising Foxp3-expressing CD25+CD4+ regulatory T cells in immunological tolerance to self and non-self. Nat Immunol. 2005; 6:345–352. [PubMed: 15785760]
24. Khong HT, Restifo NP. Natural selection of tumor variants in the generation of "tumor escape" phenotypes. Nat Immunol. 2002; 3:999–1005. [PubMed: 12407407]
25. Kim I, Moon SO, Kim SH, Kim HJ, Koh YS, Koh GY. Vascular endothelial growth factor expression of intercellular adhesion molecule 1 (ICAM-1), vascular cell adhesion molecule 1 (VCAM-1), and E-selectin through nuclear factor-kappa B activation in endothelial cells. J Biol Chem. 2001; 276:7614–7620. [PubMed: 11108718]
26. Gamble JR, Khew-Goodall Y, Vadas MA. Transforming growth factor-beta inhibits E-selectin expression on human endothelial cells. J Immunol. 1993; 150:4494–4503. [PubMed: 7683321]
27. Griffioen AW, Damen CA, Martinotti S, Blijham GH, Groenewegen G. Endothelial intercellular adhesion molecule-1 expression is suppressed in human malignancies: the role of angiogenic factors. Cancer Res. 1996; 56:1111–1117. [PubMed: 8640769]
28. Flati V, Pastore LI, Griffioen AW, et al. Endothelial cell anergy is mediated by bFGF through the sustained activation of p38-MAPK and NF-kappaB inhibition. Int J Immunopathol Pharmacol. 2006; 19:761–773. [PubMed: 17166398]
29. Hellebrekers DM, Castermans K, Vire E, et al. Epigenetic regulation of tumor endothelial cell anergy: silencing of intercellular adhesion molecule-1 by histone modifications. Cancer Res. 2006; 66:10770–10777. [PubMed: 17108113]
30. Tabruyn SP, Memet S, Ave P, et al. NF-kappaB activation in endothelial cells is critical for the activity of angiostatic agents. Mol Cancer Ther. 2009; 8:2645–2654. [PubMed: 19706735]
31. de Visser KE, Korets LV, Coussens LM. De novo carcinogenesis promoted by chronic inflammation is B lymphocyte dependent. Cancer Cell. 2005; 7:411–423. [PubMed: 15894262]
32. Menard S, Tomasic G, Casalini P, et al. Lymphoid infiltration as a prognostic variable for early-onset breast carcinomas. Clin Cancer Res. 1997; 3:817–819. [PubMed: 9815754]
33. Zhang L, Conejo-Garcia JR, Katsaros D, et al. Intratumoral T cells, recurrence, and survival in epithelial ovarian cancer. N Engl J Med. 2003; 348:203–213. [PubMed: 12529460]
34. Bromwich EJ, McArdle PA, Canna K, et al. The relationship between T-lymphocyte infiltration, stage, tumour grade and survival in patients undergoing curative surgery for renal cell cancer. Br J Cancer. 2003; 89:1906–1908. [PubMed: 14612901]
35. Schumacher K, Haensch W, Roefzaad C, Schlag PM. Prognostic significance of activated CD8(+) T cell infiltrations within esophageal carcinomas. Cancer Res. 2001; 61:3932–3936. [PubMed: 11358808]
36. DeNardo DG, Barreto JB, Andreu P, et al. CD4(+) T cells regulate pulmonary metastasis of mammary carcinomas by enhancing protumor properties of macrophages. Cancer Cell. 2009; 16:91–102. [PubMed: 19647220]

37. Ralainirina N, Poli A, Michel T, et al. Control of natural killer (NK) cell functions by CD4+CD25+ regulatory T cells. J Leukoc Biol. 2006

38. Deaglio S, Dwyer KM, Gao W, et al. Adenosine generation catalyzed by CD39 and CD73 expressed on regulatory T cells mediates immune suppression. J Exp Med. 2007; 204:1257–1265. [PubMed: 17502665]

39. Ohta A, Gorelik E, Prasad SJ, et al. A2A adenosine receptor protects tumors from antitumor T cells. Proc Natl Acad Sci U S A. 2006; 103:13132–13137. [PubMed: 16916931]

40. Dannull J, Su Z, Rizzieri D, et al. Enhancement of vaccine-mediated antitumor immunity in cancer patients after depletion of regulatory T cells. J Clin Invest. 2005; 115:3623–3633. [PubMed: 16308572]

41. Sutmuller RP, van Duivenvoorde LM, van Elsas A, et al. Synergism of cytotoxic T lymphocyte-associated antigen 4 blockade and depletion of CD25(+) regulatory T cells in antitumor therapy reveals alternative pathways for suppression of autoreactive cytotoxic T lymphocyte responses. J Exp Med. 2001; 194:823–832. [PubMed: 11560997]

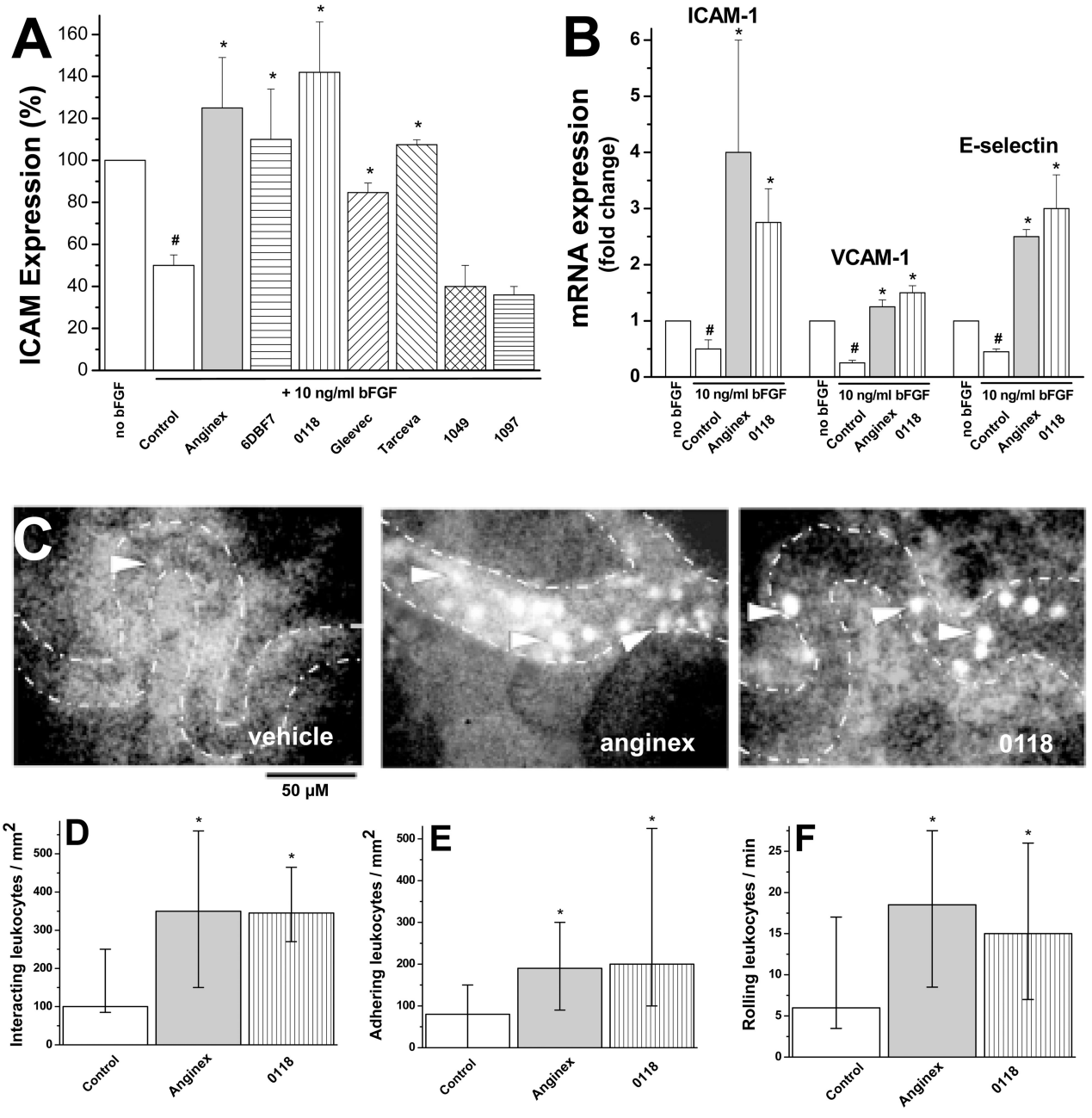

Figure 1. EAM expression and leukocyte-vessel wall interactions

(A) FACS analysis of ICAM-1 protein expression on HUVEC, with or without bFGF treatment (10 ng/ml), 3 days post treatment with 10μM of Anginex, 6DBF7, 0118, 1049, 1097 or 10μg/ml of Gleevec or Tarceva. Results shown are MFI (± SEM) of 4 independent experiments normalized to the control ($^{\#}p<0.05$ vs. no bFGF; $^{*}p<0.05$ vs. control). (B) mRNA expression of ICAM-1, VCAM-1 and E-selectin (analyzed by using quantitative real-time RT-PCR) in HUVEC treated with and without 10μM anginex or 0118. Results shown are mean values (± SEM) of 4 independent experiments, as fold changes compared to

no bFGF ($^{\#}p<0.05$ vs. no bFGF; $*p<0.05$ vs. control). (C) Images from intravital fluorescence microscopy showing rhodamine-labeled leukocytes (arrows) in microvessels (dotted lines) of B16F10 tumors from mice treated with vehicle, anginex, 0118. (D) Interacting leukocytes per mm^2 vessel surface in B16F10 tumor vessels in angiostatically treated and untreated mice. Number of adhering per mm^2 (E) and rolling per minute (F) leukocytes in tumor vessels of angiostatically treated and untreated mice. Angiostatic treatment was administered for 2 days at a dose of 10 mg/kg IP BID and imaged on day 3. For panels D–F data are presented as medians and interquartile ranges ($*p<0.05$).

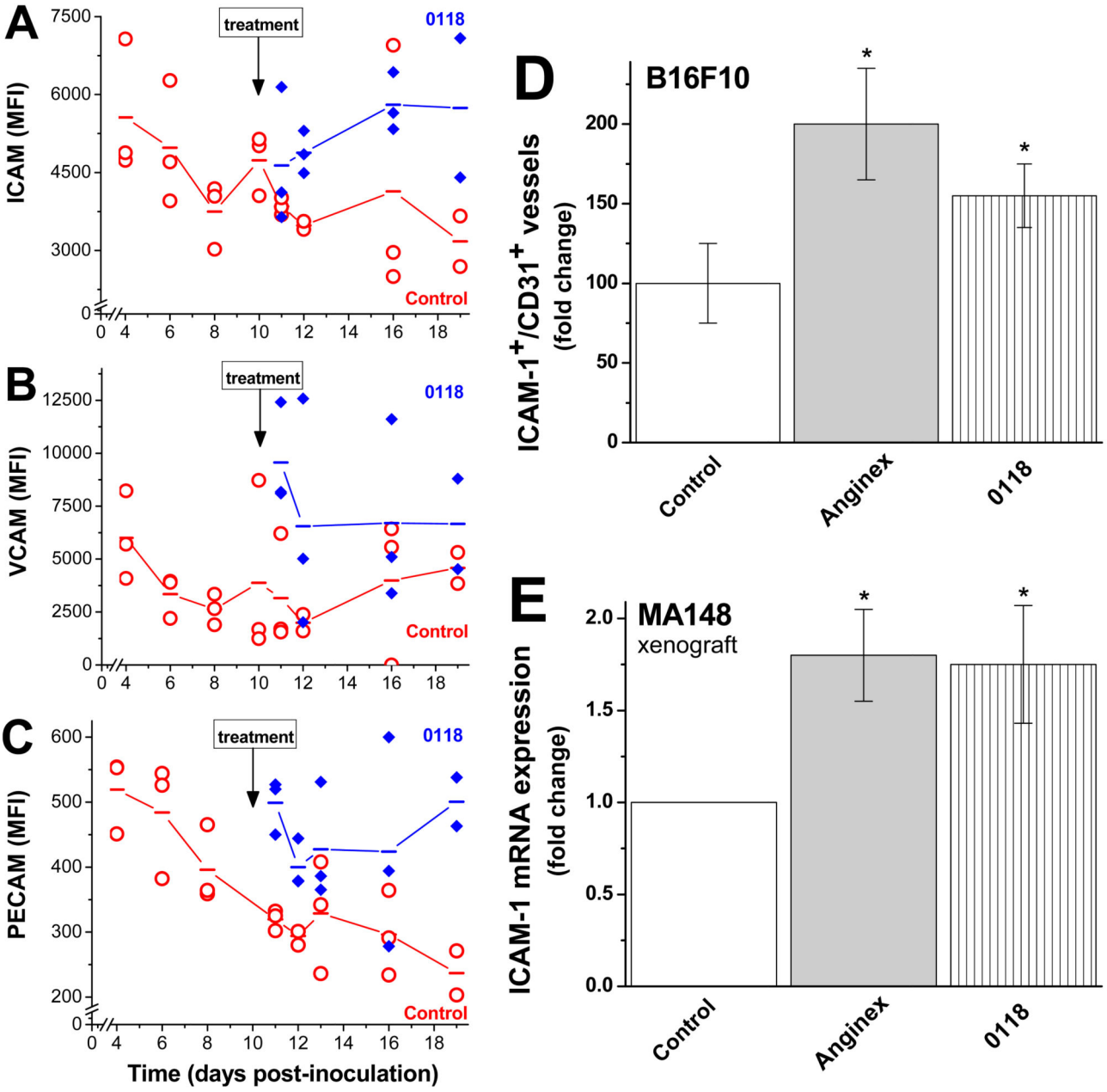

Figure 2. Time course of tumor EAM and angiostatic inhibitor intervention

Multi-color FACS analysis was used to simultaneously measure the amount of ICAM-1 (A), VCAM (B), and PECAM (C) on tumor endothelial cells during B16F10 tumor growth, as well as the effect from treatment with 0118. Treatment with 0118 (10 mg/kg IP BID) was initiated on day 10 post inoculation with cultured tumor cells. Mean fluorescence intensities (MFI) are shown for tumor-derived single cell suspensions from individual mice, and lines connect the mean values determined on each day examined. (D) Immunohistochemistry was used to quantify ICAM-1 positive vessels in B16F10 tumors of mice with or without anginex or 0118 treatment (n=6), shown as the relative mean number of ICAM-1 positive

vessels per CD31 positive vessels, as fold changes compared to untreated mice (± SEM; *p<0.05). (E) Quantitative real-time RT-PCR analysis of the effect of angiostatic treatment on expression of murine ICAM-1 expression, using mouse specific primers, in the stroma of human MA148 tumors in mice. Data are presented as the relative mean expression as fold changes compared to untreated mice (± SEM; *p<0.05).

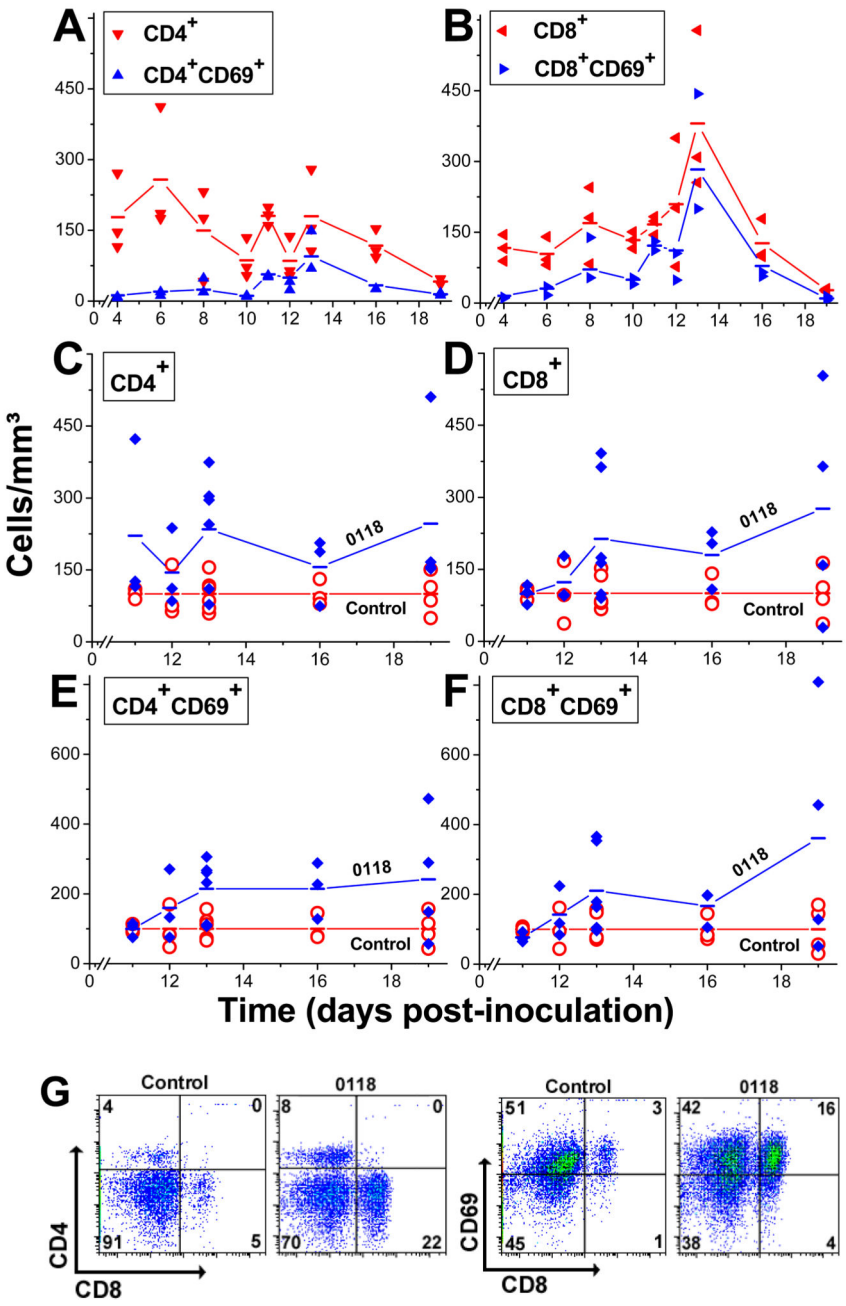

Figure 3. Changes in T cell populations during tumor growth

Multi-color FACS analysis was used to simultaneously measure changes in T cell populations in B16F10 tumors during growth. Data is shown as points for individual mice, and lines connect the mean values for $CD4^+$ and $CD4^+CD69^+$ cells (A), and $CD8^+$ and $CD8^+CD69^+$ cells (B). Relative enhancement in the number of $CD4^+$ (C), $CD8^+$ (D), $CD4^+CD69^+$ (E), and $CD8^+CD69^+$ (F) cells in tumors treated with 0118. In order to correctly compare different size tumors throughout the course of the experiment, results are

depicted as cells/mm^3. (G) Exemplary FACS analysis dot plots for control and 0118-treated B16F10 tumor-derived cell suspensions on day 13, stained for CD4, CD8, and CD69.

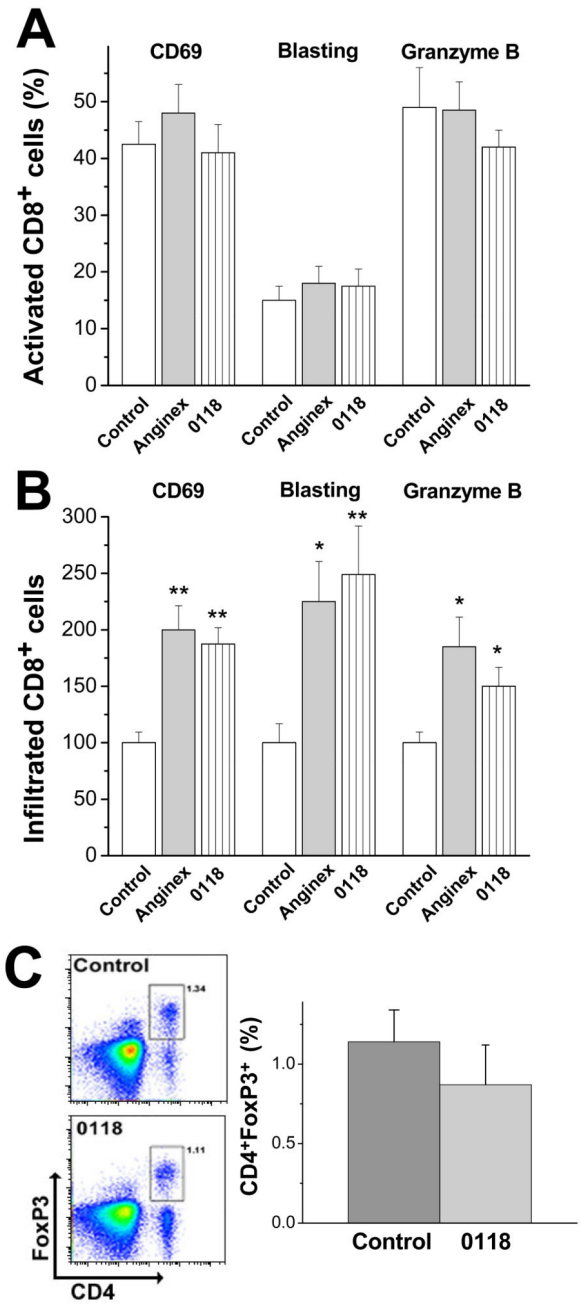

Figure 4. Infiltration of tumor-specific cytotoxic T lymphocytes

(A) Percentage of activated CD8 cells within the CD8 population (as indicated by CD69, blasting and granzyme B analysis) in untreated and treated tumors (n= 9 each). (B) Amount of activated $CD8^+$ cells in tumors treated with anginex or 0118 normalized to the control (n=9 each). Results are presented as relative mean values of 2 independent experiments (± SEM; *p<0.05, **p<0.005). (C) Exemplary flow cytometric analysis of B16F10 tumors for Tregs ($CD4^+Foxp3^+$) in untreated and 0118 treated wild type mice (left panel).

Quantification of the amount of Tregs in 0118 treated and untreated tumors (right panel; means ± SEM; n=3 each group)).

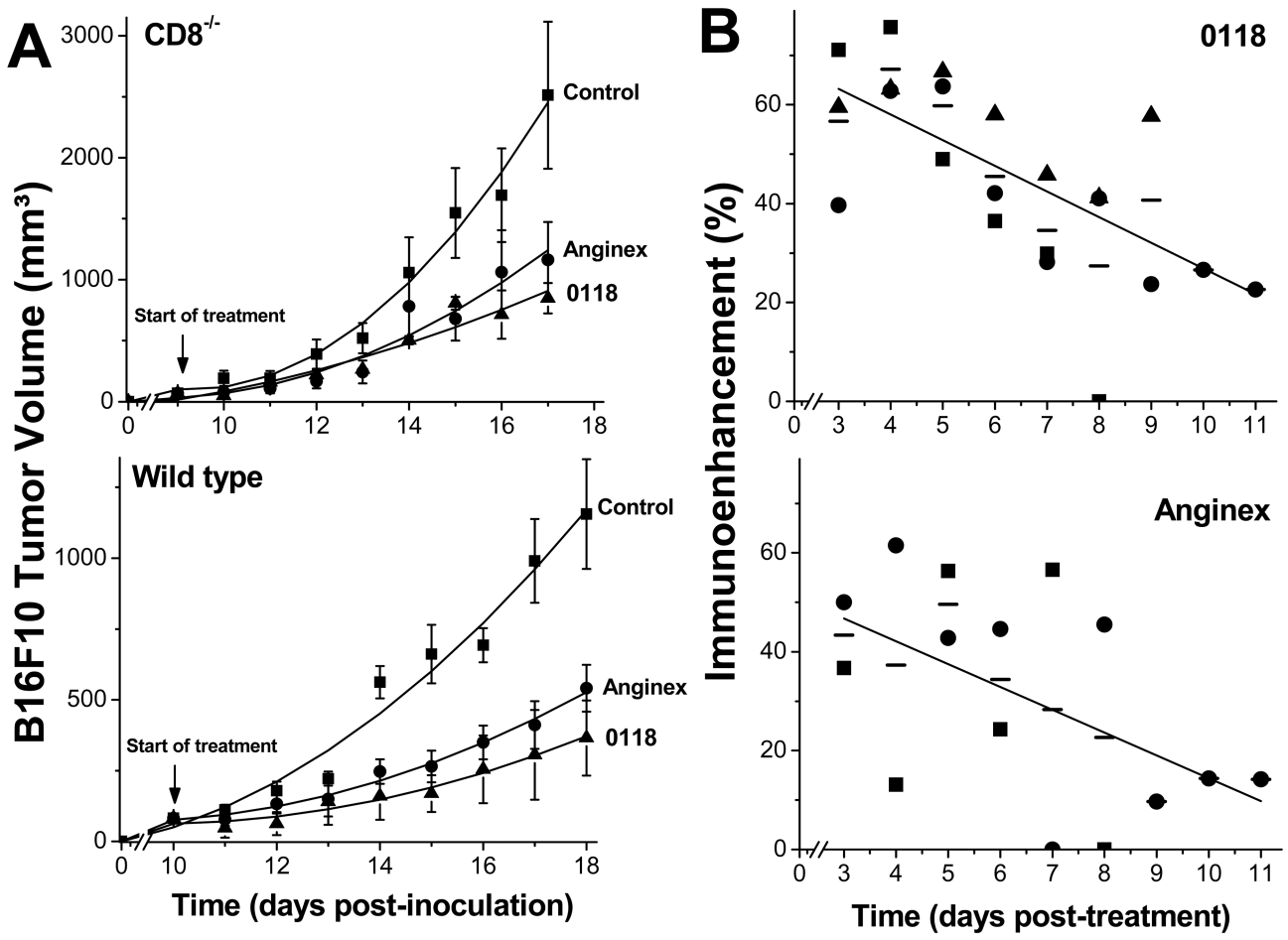

Figure 5. Immuno-extravasation enhancement effect on B16F10 tumor growth

(A) B16F10 tumor growth was monitored in $CD8^{-/-}$ and matched wild type mice treated with anginex or 0118 (both 10 mg/kg/day IP BID) compared to untreated control mice. Treatment was administered for eight days. Since tumors in null mice grew more rapidly than in wild type mice, angiostatic treatment was initiated on later days as indicated in the wild type mice, in order to run both cohorts in the study with size-matched tumors. Data are shown as the mean (± SEM) of 2 or 3 independent studies (n=12–27 per group) with polynomial trendline curve fitting. (B) *Upper panel:* 0118 induced immuno-extravasation enhancement effect on tumor growth is shown as function of time, for $CD8^{-/-}$ vs. wild type in the B16F10 model (■) and the LLC model (●), and $CD4^{-/-}$ vs. wild type in the B16F10 model (▲). The solid line represents the linear fit (R = 0.92) to all data (mean: (—)). *Lower panel:* Anginex induced immuno-extravasation enhancement effect on tumor growth is shown as function of time, for $CD8^{-/-}$ vs. wild type in the B16F10 model (■), and for $CD8^{-/-}$ vs. wild type in the LLC model (●). The solid line represents the linear fit (R = 0.90) to all data (mean: (—)). The effect from angiogenic therapy-induced immuno-extravasation enhancement effect on tumor growth was calculated by taking the daily fraction of tumor growth inhibition (i.e. the tumor size in anginex or 0118 treated mice divided by that in untreated mice) in null mice divided by the fraction of tumor growth

inhibition in wild type mice. One minus this ratio times 100 yields the percent of immuno-enhancement as shown.

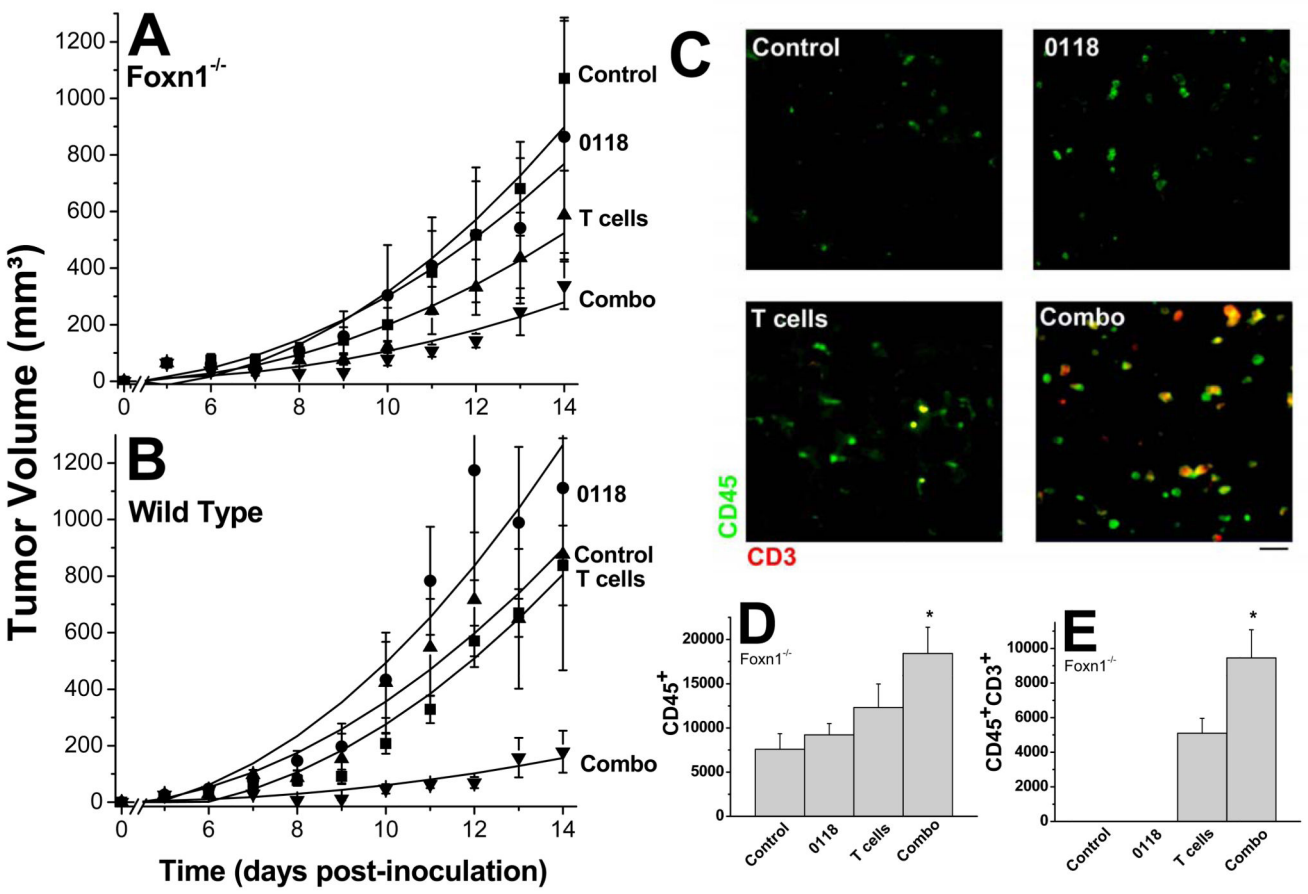

Figure 6. Adoptive T cell immunotherapy in mice

B16F10 tumor growth was monitored in T cell deficient Foxn1$^{-/-}$ (A) and wild type (B) mice treated with 0118 (10 mg/kg IP BID, days 5 and 6), transferred with T cells (2×10^7 IP, day 7), or a combination, compared to untreated control mice (n=6–16 for each group). Unlike the studies shown in Figure 6, angiostatic treatment was administered for only 2 days, for reasons discussed in the text. Data are shown as mean (± SEM) interval with polynomial trendline curve fitting (C) Exemplary immunofluorescence stainings of B16F10 tumor tissue are shown for leukocytes (CD45; green) and T cells (CD3; red) for control, 0118, T cell transferred, or combination-treated Foxn-1$^{-/-}$ mice. Quantification (mean ± SEM; *p< 0.01)) of CD45$^+$ cells (D) and CD45$^+$CD3$^+$ cells (E) in B16F10 tumors, untreated or treated with 0118, T cells, or the combination.